Thermal behaviour of polycrystalline $[Ba(H_2O)_3](ClO_4)_2$ and $[Ba(NH_3)_4](ClO_4)_2$

A. Migdał-Mikuli, J. Hetmańczyk, E. Mikuli *, Ł. Hetmańczyk

Phase Transitions Research Team, Faculty of Chemistry, Jagiellonian University, Ingardena 3, 30-060 Cracow, Poland

ABSTRACT

Phase transitions, melting processes and thermal decompositions of $[Ba(H_2O)_3](ClO_4)_2$ and $[Ba(NH_3)_4](ClO_4)_2$ were studied by differential scanning calorimetry (DSC) and thermogravimetric analysis connected with quadruple mass spectrometer (TGA/QMS). The phase transition at $T_C^h = 304.0$ K (on heating) and at $T_C^c = 286.8$ K (on cooling) was detected for $[Ba(NH_3)_4](ClO_4)_2$ by means of DSC, but none phase transition at that temperature range has been registered for $[Ba(H_2O)_3](ClO_4)_2$. The decomposition process of the $[Ba(H_2O)_3](ClO_4)_2$ supervene in the three main stages. In stage I (305–520 K) dehydration of $[Ba(H_2O)_3](ClO_4)_2$ to anhydrous $Ba(ClO_4)_2$ undergoes in two steps, in which consecutively 1/3 (at 305–360 K) and 2/3 (at 361–520 K) of all H_2O molecules are liberated. In stage II (521–740 K) anhydrous $Ba(ClO_4)_2$ has two solid–solid phase transitions: at $T_{C1} = 566.6$ K and at $T_{C2} = 641.7$ K. Next it melts at $T_m = 760$ K. Stage III (above 761 K) is connected with decomposition and explosion of melted $Ba(ClO_4)_2$. The decomposition process of the $[Ba(NH_3)_4](ClO_4)_2$ supervene in the three main stages, too. Stage I (310–520 K) is connected with deammination of $[Ba(NH_3)_4](ClO_4)_2$ to $Ba(ClO_4)_2$ and all NH_3 molecules are liberated. Stages II and III (521–850 K) are exactly the same as they were observed for $[Ba(H_2O)_3](ClO_4)_2$.

© 2009 Elsevier B.V. All rights reserved.

1. Introduction

Melting and thermal decomposition processes of several aquametal(II) and amminemetal(II) chlorates(VII) (later called perchlorates) have been investigated by us up to now [1–7]. The thermal decomposition of the anhydrous barium perchlorate has been measured by Zinov'ev and Chudinova [8] and by Acheson and Jacobs [9]. According to them, $Ba(ClO_4)_2$ decomposes in the temperature range of 708–768 K to the final products: oxygen and solid barium chloride. In addition, barium perchlorate has two structural phase transitions in the temperature range of 298–650 K. The transition from α-phase to β-phase occurs at $T_{C2} = 557$ K and that from β-phase to γ-phase at $T_{C1} = 633$ K [9,10]. The decomposition of anhydrous barium perchlorate was not followed after melting of the sample. A differential thermal analysis (DTA) study of $[Ba(H_2O)_3](ClO_4)_2$ shows that dehydration of this compound to anhydrous $Ba(ClO_4)_2$ undergoes in two steps in the temperature range of 330–530 K. The first two molecules of water per formula unit are liberated in the temperature range of 336–406 K (two stage process is not clearly separated), and then compound loss of the final one molecule H_2O in the temperature range of 420–530 K [9].

The crystal structure of $[Ba(H_2O)_3](ClO_4)_2$ at room temperature (RT) is hexagonal, P6_3/m, $a = 7.277(2)$ Å, $c = 9.656(1)$ Å,

$V = 442.9(1)$ Å^3 [11]. The RT crystal structure of $[Ba(NH_3)_4](ClO_4)_2$ is unknown. Our preliminary X-ray measurements indicate that it has regular structure, Fm3m.

Unfortunately, there is still lack of the data in the literature concerning thermal decomposition process of amminemetal(II) and aquametal(II) perchlorates. As a natural extension of those studies we present here the results for $[Ba(H_2O)_3](ClO_4)_2$ and $[Ba(NH_3)_4](ClO_4)_2$.

The general aim of these studies was to gain a better understanding of mechanisms of thermal decomposition of the triaquabarium perchlorate and tetraamminebarium perchlorate, particularly of the dehydration and deammination processes, respectively. We would like also to make a comparison between the results obtained for these both compounds and to compare obtained results for $[Ba(H_2O)_3](ClO_4)_2$ with those for $[Ca(H_2O)_4](ClO_4)_2$ and also with those for other aqua complexes, namely: $[M(H_2O)_6](ClO_4)_2$ compounds, where M = Mg, Ni, Mn, Fe, Co, Cu, Zn, Cd and Hg. We would like also to drawn more general conclusions of the role which pay different ligands coordinated to different metals on thermal decomposition process of the ionic coordinated compounds of this type. It is interesting to check out how the crystals structure influences on their thermal properties, too.

In addition we wanted to investigate the polymorphism of $[Ba(H_2O)_3](ClO_4)_2$ and $[Ba(NH_3)_4](ClO_4)_2$, in the temperature range of 233–333 K, calculate the thermodynamics parameters and to compare the results with those obtained earlier for other aquametal(II) and amminemetal(II) perchlorates [5,12–16], respectively.

* Corresponding author. Tel.: +48 12 6632256; fax: +48 12 6340515.
E-mail address: mikuli@chemia.uj.edu.pl (E. Mikuli).

2. Experimental

The [Ba(H$_2$O)$_3$](ClO$_4$)$_2$ was purchased from Aldrich Chemical Company, Inc. and used without further purification. Second compound: [Ba(NH$_3$)$_4$](ClO$_4$)$_2$ was obtained from triaquabarium perchlorate. The triaquabarium perchlorate complex was placed in a quartz vessel and put in a glass tube, through which dry gaseous ammonia was blown, and the tube was placed in an oven, according to the method proposed by Smith and Koch [17]. First the tube was heated for several days up to about 400 K until all the water from [Ba(H$_2$O)$_3$](ClO$_4$)$_2$ was lost and [Ba(NH$_3$)$_4$](ClO$_4$)$_2$ was composed. Then, after cooling the tube to the room temperature, the obtained compound was put into a desiccator for several hours in order to get rid of ammonia excess.

Before the measurements were taken, the composition of the compounds under study was determined based on its barium and ammonia content by titration using EDTA and HCl, respectively. The average barium content was found to be equal to the theoretical value within an error margin of ca0.3% for [Ba(H$_2$O)$_3$](ClO$_4$)$_2$ and of ca. 1% for [Ba(NH$_3$)$_4$](ClO$_4$)$_2$. The average content of NH$_3$ was found to be equal to the theoretical values within the error limit of ca. 2%.

Fourier transforms middle-infrared absorption measurements (FT-MIR) were performed using a *Bruker EQUINOX-55* spectrometer. The FT-MIR measurements at room temperature were performed in the frequency range of 4000–400 cm^{-1} with a resolution of 2 cm^{-1}. Title powdered compounds were mixed with Nujol and drifted on KBr pellet.
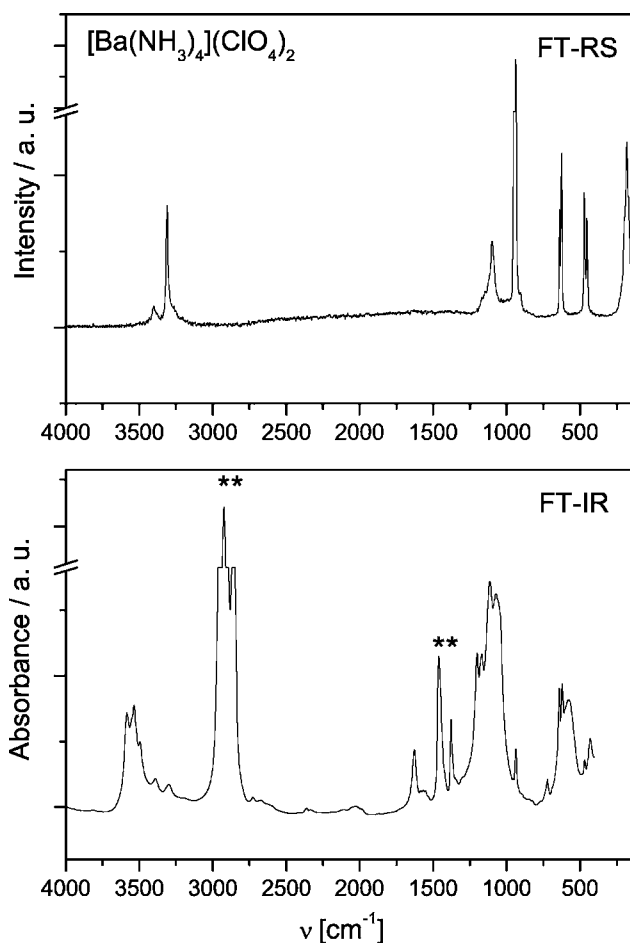

Fig. 1. Comparison of the room temperature Raman and infrared spectra of [Ba(H$_2$O)$_3$](ClO$_4$)$_2$.

Fig. 2. Comparison of the room temperature Raman and infrared spectra of [Ba(NH$_3$)$_4$](ClO$_4$)$_2$.

Fourier transforms Raman scattering measurements (FT-RS) were performed at room temperature with a *Bio-Rad* spectrometer, resolution 4 cm^{-1}. The incident radiation ($\lambda = 1064$ nm) was from the Neodymium laser YAG Spectra-Physics.

Figs. 1 and 2 present the comparison of FT-MIR and FT-RS room temperature spectra of [Ba(H$_2$O)$_3$](ClO$_4$)$_2$ and [Ba(NH$_3$)$_4$](ClO$_4$)$_2$, respectively. The list of the band positions of the Raman and infrared spectra at room temperature and their assignments for both investigated compounds are presented in Table 1. Assignments of the bands of all spectra are in a good agreement with the literature data [18–21]. Besides of chemical analysis the obtained spectra confirmed proper composition of the investigated compounds.

The thermogravimetric analyses (TGA) with simultaneous differential thermal analyses (SDTA) measurements were performed using a *Mettler-Toledo 851^e* apparatus. Samples of masses equal to 18.3841 mg of [Ba(H$_2$O)$_3$](ClO$_4$)$_2$ and 14.6645 mg of [Ba(NH$_3$)$_4$](ClO$_4$)$_2$ were placed in 150 μl platinum crucibles. The measurements were made in a flow of Argon (60 ml min^{-1}), within temperature range of 305–774 K and 310–774 K for [Ba(H$_2$O)$_3$](ClO$_4$)$_2$ and [Ba(NH$_3$)$_4$](ClO$_4$)$_2$, respectively. The TGA measurements were performed at a constant heating rate of 10 K min^{-1}. The simultaneous evolved gas analysis (SEGA) was performed during the experiments by a joined on-line quadruple mass spectrometer (QMS) using a *Thermostar-Balzers* apparatus. The temperature was measured by a Pt–Pt/Rh thermocouple with an accuracy of ±0.5 K.

The DSC measurements in temperature range of 300–873 K were performed using a *Mettler-Toledo 821^e* calorimeter. The samples
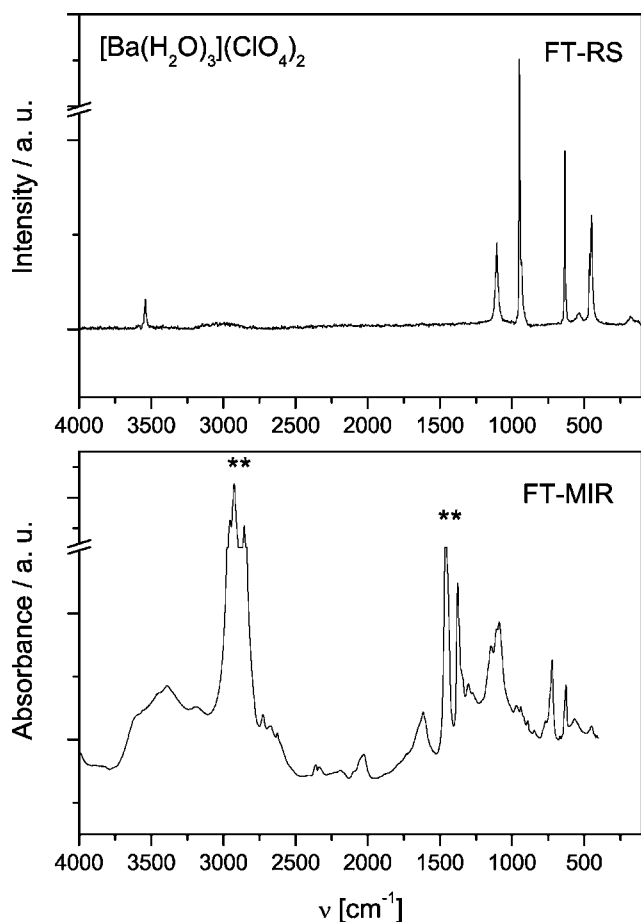
Table 1
List of band positions of the Raman (FT-RS) and infrared (FT-MIR) spectra of $[Ba(H_2O)_3](ClO_4)_2$ and $[Ba(NH_3)_4](ClO_4)_2$ at room temperature.

$[Ba(H_2O)_3](ClO_4)_2$			$[Ba(NH_3)_4](ClO_4)_2$		
Frequencies in cm^{-1}		Assignments	Frequencies in cm^{-1}		Assignments
RS	IR		RS	IR	
3583 vw	3597 sh	$\nu_{as}(OH)$		3585 s	$\nu_{as}(NH)$
				3536 s	$\nu_s(NH)$
3542 w	3448 sh	$\nu_s(OH)$		3495 sh	$\nu_s(NH)$
	3391 br	$\nu_s(OH)$	3402 m	3391 m	$\nu_{as}(NH)$
			3311 s		$\nu_s(NH)$
	3192 w	$2\delta_{as}(HOH)$	3264 w	3298 m	$2\delta_{as}(HNH)$
	1616 s	$\delta_{as}(HOH)$		1628 s	$\delta_{as}(HNH)$
	1295 m	$\delta_s(HOH)$		1200 s	$\delta_s(HNH)$
	1144 s	$\nu_{as}(ClO)F_2$	1150 sh	1169 s	$\nu_{as}(ClO)F_2$
1105 s	1097 s	$\nu_{as}(ClO)F_2$	1098 m	1114 vs	$\nu_{as}(ClO)F_2$
	1090 s	$\nu_{as}(ClO)F_2$		1069 vs	$\nu_{as}(ClO)F_2$
948 vs	952 w	$\nu_s(ClO)A$	949 vs		$\nu_s(ClO)A$
	929 w	$2\delta(OClO)E$	938 vs	937 s	$2\delta(OClO)E$
	884 w	$\rho_r(H_2O)$	905 sh		$\rho_t(NH_3)$
	723 s	$\rho_t(H_2O)$		722 m	$\rho_r(NH_3)$
	669 sh	$\delta_d(OClO)F_2$	640 s	641 s	$\delta_d(OClO)F_2$
634 vs	627 s	$\delta_d(OClO)F_2$	626 s	620 s	$\delta_d(OClO)F_2$
535 m	567 m	$\nu_s(BaO)$		576 s	$\nu_{as}(BaN)$
461 sh		$\delta_d(OClO)E$	471 s	469 w	$\delta_d(OClO)E$
450 s	446 m	$\delta_d(OClO)E$	454 s	430 m	$\delta_d(OClO)E$
180 w		$\nu_L(lattice)$	182 s		$\nu_L(lattice)E$
			127 m		$\nu_L(lattice)E$

vs, very sharp; s, sharp; m, medium; sh, shoulder; w, weak; vw, very weak.

of masses equal to 8.61 mg for $[Ba(H_2O)_3](ClO_4)_2$ and 3.33 mg for $[Ba(NH_3)_4](ClO_4)_2$ were placed in 40 μl aluminum partially open crucibles (micro hole preserves constant pressure over the sample). Measurements were performed under constant flow of Argon (80 ml min^{-1}) with the heating rate equals to 10 K min^{-1}. DSC measurements in temperature range of 233–333 K were performed using a *Mettler-Toledo 821^e* calorimeter too.

3. Results and discussion

3.1. DSC measurements for $[Ba(H_2O)_3](ClO_4)_2$ and $[Ba(NH_3)_4](ClO_4)_2$ in the temperature range of 233–333 K

The DSC measurements were performed both on heating and cooling a samples of masses equal to: 7.62 mg for $[Ba(NH_3)_4](ClO_4)_2$ and 19.06 mg for $[Ba(H_2O)_3](ClO_4)_2$, in both cases at constant scanning rate of 10 K min^{-1} in the temperature range of 233–333 K. Fig. 3a and b shows the temperature dependencies of the heat flow (DSC curves) obtained while heating (lower curve) and while cooling (upper curve) of the $[Ba(NH_3)_4](ClO_4)_2$ and of the $[Ba(H_2O)_3](ClO_4)_2$ samples, respectively. One can see in Fig. 3a that in the above-mentioned temperature range $[Ba(NH_3)_4](ClO_4)_2$ possesses phase transition in solid state. One anomaly on each of these DSC curves was registered at $T_C^h = 304.0$ K (on heating) and at $T_C^c = 286.8$ K (on cooling). The presence of ca. 17.2 K hysteresis of the phase transition temperature at T_C and the heat flow anomaly sharpness suggest that the detected phase transition is a first-order one. The thermodynamic parameters of the detected phase transition are presented in Table 2. The investigated by us earlier [11–14] crystalline compounds of the type $[M(NH_3)_6](ClO_4)_2$, where M = Ni, Mg, Ca, Co, Cd, also possess one or two solid–solid phase transitions. The difference is that phase transitions registered for these compounds are observed in the low temperature region (temperature range of 100–290 K). None of the above mentioned compounds exhibit phase transitions in the temperature close to 300 K.

As can be seen in Fig. 3b none anomaly on DSC curve for $[Ba(H_2O)_3](ClO_4)_2$ was observed. It is different situation than in the case of investigated earlier by us $[M(H_2O)_6](ClO_4)_2$ compounds
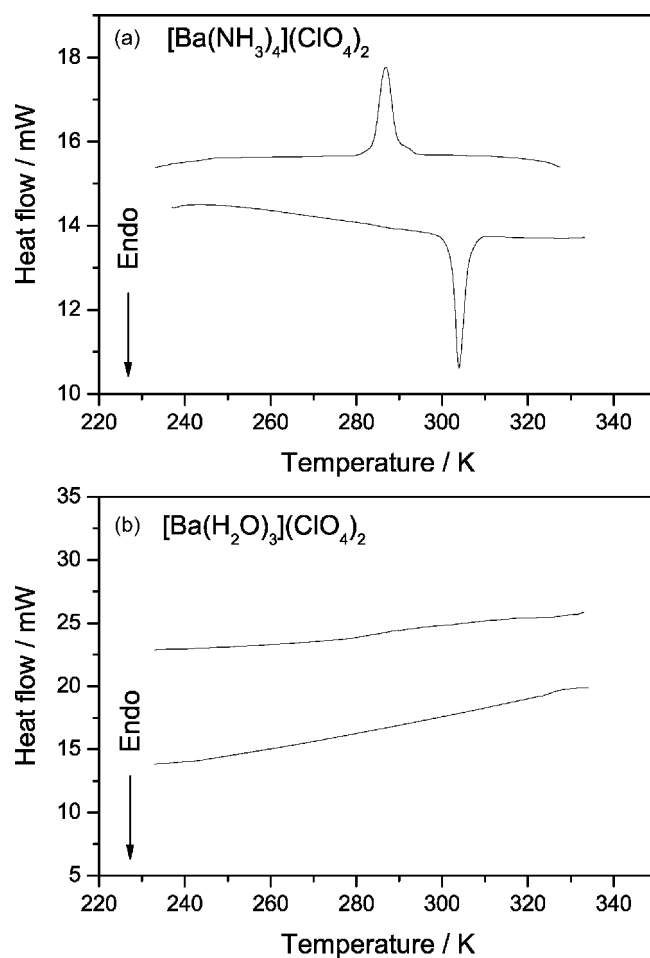

Fig. 3. DSC curves registered on heating and cooling of $[Ba(NH_3)_4](ClO_4)_2$ (a) and for $[Ba(H_2O)_3](ClO_4)_2$ (b) samples in the temperature range of 233–333 K at a rate of 10 K min^{-1}.

Table 2
Thermodynamic parameters of the phase transitions of $[Ba(NH_3)_4](ClO_4)_2$.

	T_C (K)	$\Delta H \pm \Delta \delta H$ (kJ/mol)	$\Delta S \pm \Delta \delta S$ (kJ/mol K)
Heating	304.0 ± 0.1	3.27 ± 0.09	10.74 ± 0.30
Cooling	286.8 ± 0.1	2.84 ± 0.02	9.89 ± 0.08

(M = Mg, Mn, Fe, Co, Ni, Cu, Zn, Cd, Hg and Ca) [3–5,15], which possess several phase transitions in the solid state in the discussed temperature range.

3.2. Thermal behaviour of $[Ba(H_2O)_3](ClO_4)_2$ and $[Ba(NH_3)_4](ClO_4)_2$ in the temperature range of 300–873 K

Fig. 4a and b shows the DSC results obtained in the temperature range of 300–873 K with the scanning rate of 10 K min^{-1} for $[Ba(H_2O)_3](ClO_4)_2$ and $[Ba(NH_3)_4](ClO_4)_2$ samples, respectively, in non-hermetically closed aluminum vessel.

Four very broad endothermic peaks at ca. 350 K, 384 K, 421 K and 476 K can be observed in Fig. 4a. In fact the fourth peak being the overlap of at least four processes. Peaks at 350 K and 384 K, 421 K can be interpreted as connected with the sample dehydration, what will be proved below by means of the TGA results. The process of the dehydration undergoes according to the following reactions:
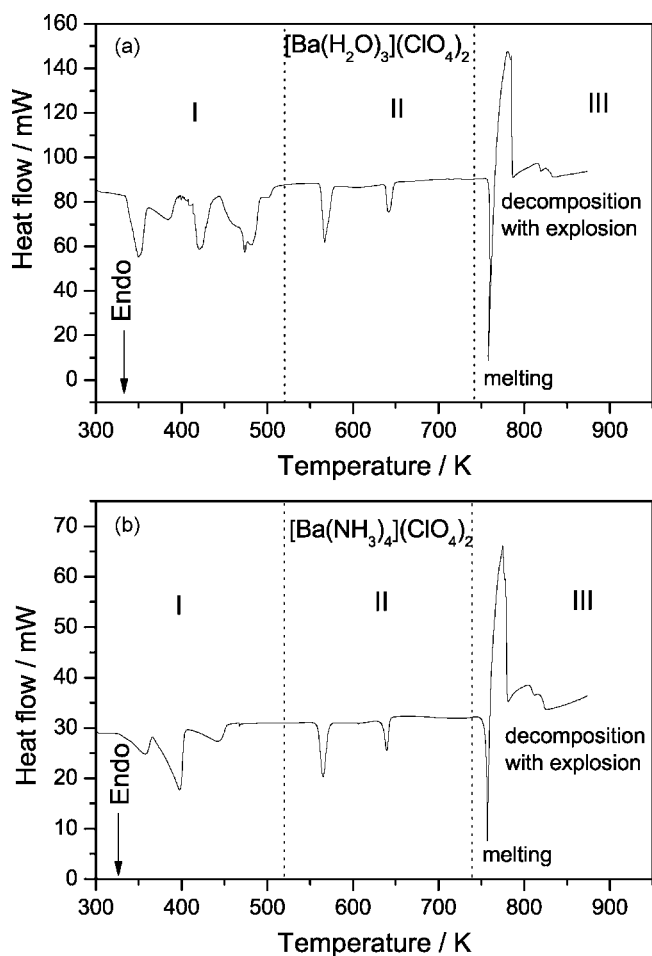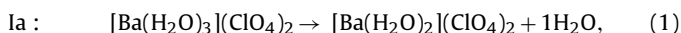
$$\text{Ia}: \qquad [Ba(H_2O)_3](ClO_4)_2 \rightarrow [Ba(H_2O)_2](ClO_4)_2 + 1H_2O, \qquad (1)$$

$$\text{Ib}: \qquad [Ba(H_2O)_2](ClO_4)_2 \rightarrow Ba(ClO_4)_2 + 2H_2O. \qquad (2)$$

Fig. 4. DSC curves for $[Ba(H_2O)_3](ClO_4)_2$ (a) and for $[Ba(NH_3)_4](ClO_4)_2$ (b) in the range of 300–873 K. The vertical dashed line denotes temperature above which anhydrous $Ba(ClO_4)_2$ is formed in both cases.

Step Ia undergoes at ca. 350 K but in fact step Ib is double (at ca. 384 K and 421 K) what is clearly seen from thermogravimetric analysis presented below. It should be pointed out that the dehydration process of $[Ba(H_2O)_3](ClO_4)_2$ is quite different from the dehydration processes registered for $[Ca(H_2O)_4](ClO_4)_2$ and compounds of the type: $[M(H_2O)_6](ClO_4)_2$, where M = Mg, Ni, Mn, Fe, Co, Cu, Zn, Cd and Hg. All of these perchlorates dissolve in its own coordination water (melts) before the dehydration. The broad and overlapped endothermic peak registered at ca. 476 K in the DSC curve for $[Ba(H_2O)_4](ClO_4)_2$ is most probably connected with dissolving, of anhydrous $Ba(ClO_4)_2$ in the water (steam), which was just released from $[Ba(H_2O)_4]^{2+}$. The released water does not evaporate very quickly from crucible and can step by step interact with the solid sample, because aluminum crucible possesses a micro-hole. This micro-hole additionally preserves that this process undergoes at a constant pressure. A group of endothermic peak appears as a consequence of this piecemeal dissolving. It should be noticed that $Ba(ClO_4)_2$ is very well soluble in water. It is a reason why we cannot observe similar peak in the DSC curve registered for $[Ba(NH_3)_4](ClO_4)_2$. Two endothermic peaks registered in DSC curve at 566.6 K and 641.7 K are connected with the two phase transitions in the solid phase of $Ba(ClO_4)_2$. Successive endothermic peak on DSC curve at 760 K corresponds to melting of anhydrous compound (melting in Fig. 4a and b). The last broad and large exothermic peak (at 780 K) can be explained as connected with the process of the $Ba(ClO_4)_2$ decomposition and explosion. This is in a good agreement with the data for anhydrous barium perchlorate obtained by Acheson and Jacobs [9], but according to them, $Ba(ClO_4)_2$ decomposes without melting. However, it is known from the data included in MSDS (Material Safety Data Sheet, Sigma–Aldrich) that the temperature of melting point of $Ba(ClO_4)_2$ equals to ca. 778 K.

Three endothermic peaks clearly visible on DSC curve for $[Ba(NH_3)_4](ClO_4)_2$ in the temperature range of 300–520 K (Fig. 4b) are connected with piecemeal liberation of all NH$_3$ ligands which undergoes at least in three steps. Complete process of deammination undergoes according to the following reactions:

$$\text{I}: \qquad [Ba(NH_3)_4](ClO_4)_2 \rightarrow Ba(ClO_4)_2 + 4NH_3. \qquad (3)$$
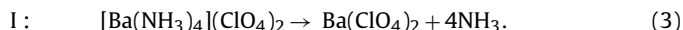
Endothermic peaks registered in DSC curve at 565.3 K and 639.7 K are connected with the phase transitions in solid state of $Ba(ClO_4)_2$. Successive endothermic peak present in DSC curve at 760 K corresponds similarly to melting of $Ba(ClO_4)_2$, as former. The last large and broad exothermic peak (at 775 K) can be explained as connected with the process of the $Ba(ClO_4)_2$ decomposition and explosion.

Fig. 5 shows TGA, DTG and QMS curves recorded for $[Ba(H_2O)_3](ClO_4)_2$ at a constant heating rate of 10 K min^{-1} in the temperature range of 305–774 K. During the TGA experiment, the QMS spectra of masses were followed from $m/e = 1$–100, however, for reasons of graphic readability, only the masses of $m/e = 16$, 17, 18 and 32 – representing: O, OH, H$_2$O and O$_2$ – are shown. The TGA, DTG and QMS curves show that the decomposition of the sample proceeds in three main stages (I, II and III). It can be observed that the first stage involves freeing all of H$_2$O molecules. The dehydration undergoes in the two steps (Ia and Ib). Statistically at step Ia one molecule of water per one formula unit is freeing and the rest two molecules of water are freeing at step Ib. Summary, in the temperature range of 305–520 K all molecules of water are freeing and the anhydrous $Ba(ClO_4)_2$ is formed. In the temperature range of 520–740 K (stage II) the investigated anhydrous compound $Ba(ClO_4)_2$ has two phase transitions in solid phase at $T_{C1} = 566.6$ K and at $T_{C2} = 641.7$ K and then melts at $T_m = 760$ K. The third stage is connected with the decomposition of resulting $Ba(ClO_4)_2$ to oxygen and solid $BaCl_2$. The temperatures, percentage mass of losses and the products of the decomposition of $[Ba(H_2O)_3](ClO_4)_2$ at particular stages are presented in Table 3.

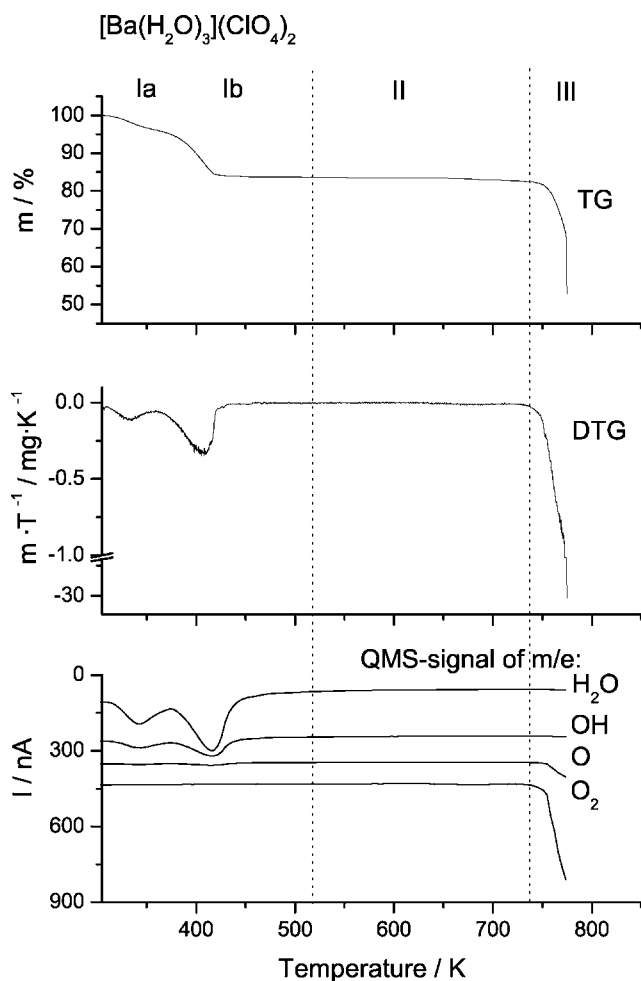**Fig. 5.** TGA, DTG and QMS curves for $[Ba(H_2O)_3](ClO_4)_2$ in the range of 305–774 K, at a constant heating rate of $10\,K\,min^{-1}$.

Fig. 6. TGA, DTG and QMS curves for $[Ba(NH_3)_4](ClO_4)_2$ in the range of 310–774 K, at a constant heating rate of $10\,K\,min^{-1}$.

Fig. 6 shows TGA, DTG and QMS curves recorded for $[Ba(NH_3)_4](ClO_4)_2$ at a constant heating rate of $10\,K\,min^{-1}$ in the temperature range of 310–774 K. During the TGA experiment, the QMS spectra of masses were followed from $m/e = 1$–100, however, for reasons of graphic readability, only the masses of $m/e = 14$, 15, 16, 17 and 32 – representing: N, NH, NH_2/O, NH_3 and O_2 – are shown. The TGA, DTG and QMS curves show that the decomposition of the
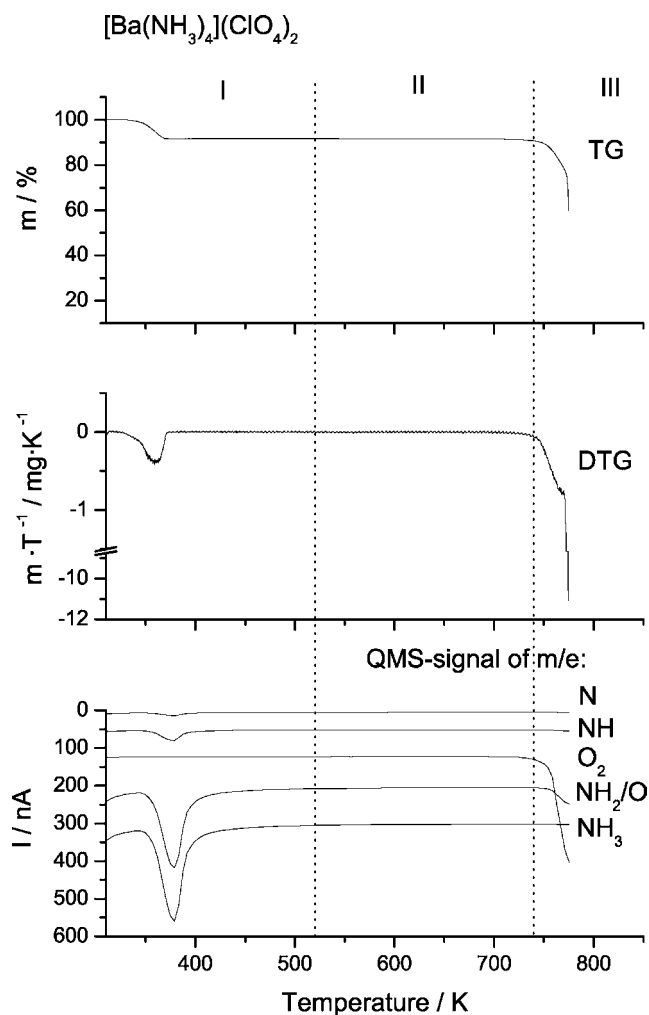
sample proceeds in three main stages too (I, II and III). In the temperature range of 310–488 K two molecules of ammonia are freeing and the anhydrous $Ba(ClO_4)_2$ is formed. The other two NH_3 ligands are released before 310 K as the sample is very unstable. We were not able to reach temperatures lower than 310 K in our TGA measurements condition. In the temperature range of 520–740 K (stage

Table 3
Parameters of $[Ba(H_2O)_3](ClO_4)_2$ thermal analysis.

Stage number	Temperature range (K)	Mass loss at the stage (%)	Calculated values (%)	Products of decomposition
Ia	305–360	4.7	4.6	1 H_2O
Ib	361–520	10.9	9.2	2 H_2O
II	521–740	0	0	
III	760	Melting of $Ba(ClO_4)_2$		
	761–850	Decomposition of $Ba(ClO_4)_2$ with explosion		

Initial sample mass equalled to 18.3841 mg.

Table 4
Parameters of $[Ba(NH_3)_4](ClO_4)_2$ thermal analysis.

Stage number	Temperature range (K)	Mass loss at the stage (%)	Calculated values (%)	Products of decomposition
0	Below 310	–[a]	8.4	2 NH_3 [a]
I	310–520	8.4	8.4	2 NH_3
II	521–740	0	0	
III	760	Melting of $Ba(ClO_4)_2$		
	761–850	Decomposition of $Ba(ClO_4)_2$ with explosion		

[a] These two NH_3 molecules per formula unit were not registered during this measurement because the sample is very unstable and they had been released before 300 K.

II) the investigated anhydrous compound $Ba(ClO_4)_2$ has two phase transitions in solid state at $T_{C2} = 565.3$ K and at $T_{C1} = 639.7$ K then melts at $T_m = 757$ K. The third stage is connected with decomposition of resulting $Ba(ClO_4)_2$. The temperatures, percentage mass of losses and the products of the decomposition of $[Ba(NH_3)_4](ClO_4)_2$ at particular stages are presented in Table 4. During the explosive decomposition same part of the sample was ejected from the platinum crucibles. Thus, we were not able to determine products of the decomposition anhydrous barium perchlorate but according to [8,9] $Ba(ClO_4)_2$ decomposes with formation of $BaCl_2$ and production of oxygen.

Up to now from all known perchlorates of aquametal(II) complexes only for $[Ni(H_2O)_6](ClO_4)_2$ and for $[Ca(H_2O)_4](ClO_4)_2$ the TGA curves were registered in the temperature range of 300–700 K [6,7]. Thus we were able to compare these results with obtained by us for $[Ba(H_2O)_3](ClO_4)_2$. Thermal decomposition of $[Ba(H_2O)_3](ClO_4)_2$ is somewhat different than this of $[Ni(H_2O)_6](ClO_4)_2$ [5,6]. In the temperature range of 300–520 K $[Ni(H_2O)_6](ClO_4)_2$ is losing of three water molecules per formula unit and $[Ni(H_2O)_3](ClO_4)_2$ is formed. Further process of the decomposition of triaquanickel(II) perchlorate leads directly to the final products (O_2, Cl_2 and NiO is the solid remainder of this process), without the formation of $Ni(ClO_4)_2$ as an intermediate product. In the case of $[Ba(H_2O)_3](ClO_4)_2$ the decomposition is followed by the formation of anhydrous $Ba(ClO_4)_2$, which firstly has two phase transitions in solid state, and next melts and finally decomposes to the final products $BaCl_2$ with oxygen releasing. The thermal decomposition process of $[Ba(H_2O)_3](ClO_4)_2$ is more similar to that one for $[Ca(H_2O)_4](ClO_4)_2$ [7]. Namely, both of them start loosing all molecules of water in the first stage and next anhydrous products are formed ($Ba(ClO_4)_2$ and $Ca(ClO_4)_2$, respectively). In turn, these anhydrous products firstly melt and just next decompose to the final products ($BaCl_2$ and $CaCl_2$, respectively).

Comparing the thermal decomposition processes of $[Ba(NH_3)_4](ClO_4)_2$ and $[Ca(NH_3)_6](ClO_4)_2$ [7], registered at a constant heating rate in a flow of Argon, we noticed that they proceed in an almost identical way. The main difference is in the temperature range in which all molecules of ammonia are freeing. It can be seen that in case of $[Ba(NH_3)_4](ClO_4)_2$ the particular NH_3 ligands are liberated in a much lower temperature (300–520 K) than the NH_3 in $[Ca(NH_3)_6](ClO_4)_2$ (341–601 K).

4. Conclusions

The results obtained in this work and their comparison with the literature data has led us to the following conclusions:

1. The DSC measurements of $[Ba(NH_3)_4](ClO_4)_2$ performed in the temperature range of 233–333 K allowed *one* solid–solid phase transition to be detect. The temperature of this phase transition amount to: $T_C^h = 304.0$ K (on heating) and at $T_C^c = 286.8$ K (on cooling). The large thermal hysteresis ($\Delta T \approx 17$ K) of this phase transition and the heat flow anomaly sharpness suggests that

the detected phase transition is of the first-order one. In the same temperature range $[Ba(H_2O)_3](ClO_4)_2$ has *none* phase transitions.

2. The thermal decomposition of both title compounds is similar and proceeds in three main stages. In both cases first stage is connected with a loss of the ligands (H_2O or NH_3). Dehydration of $[Ba(H_2O)_3](ClO_4)_2$ to anhydrous $Ba(ClO_4)_2$ undergoes in stage I (305–520 K) in two steps, in which consecutively 1/3 (at 305–360 K) and 2/3 (at 361–520 K) of all H_2O molecules are liberated. Deammination of $[Ba(NH_3)_4](ClO_4)_2$ to $Ba(ClO_4)_2$ starts just at 310 K and completely undergoes in stage I (310–520 K). It can be noticed that NH_3 ligands are a bit easer cleaved from central metal atoms (barium) than H_2O ligands. Two next two steps are almost identical. In the second stage anhydrous $Ba(ClO_4)_2$ undergoes two structural phase transitions in the solid state at $T_{C2} \approx 566$ K and at $T_{C1} \approx 641$ K and next it melts at ca. 758 K. The third stage (above 770 K) is connected with explosion and decomposition of barium perchlorate to oxygen and solid $BaCl_2$.

3. The thermal decomposition process of $[Ba(H_2O)_3](ClO_4)_2$ is very similar to that one of $[Ca(H_2O)_4](ClO_4)_2$ and in turn thermal decomposition process of $[Ba(NH_3)_4](ClO_4)_2$ is very similar to that one of $[Ca(NH_3)_6](ClO_4)_2$.

4. Room temperature crystal structure has small influence on thermal decomposition processes of aqua and ammine metal ionic complexes.

References

[1] M. Rachwalska, T. Stanek, Phys. Stat. Sol. (a) 48 (1978) 297–300.
[2] E. Mikuli, A. Migdał-Mikuli, M. Rachwalska, T. Stanek, Physica B 104 (1981) 326–330.
[3] E. Mikuli, A. Migdał-Mikuli, J. Mayer, Mol. Crys. Liq. Cryst. C: Mol. Mater. 8 (1997) 273–280.
[4] E. Mikuli, A. Migdał-Mikuli, J. Mayer, Mol. Crys. Liq. Cryst. C: Mol. Mater. 9 (1998) 205–215.
[5] E. Mikuli, A. Migdał-Mikuli, J. Mayer, J. Thermal Anal. 54 (1998) 93–102.
[6] M. Rachwalska, D. Majda, J. Thermal Anal. Calorim. 89 (2007) 277–281.
[7] A. Migdał-Mikuli, J. Hetmańczyk, J. Thermal Anal. Calorim. 91 (2008) 529–534.
[8] A.A. Zinov'ev, L.I. Chudinova, Zh. Neorg. Khim. 1 (1956) 1722–1730.
[9] R.J. Acheson, P.W.M. Jacobs, Can. J. Chem. 47 (1969) 3031–3039.
[10] A.A. Zinov'ev, L.I. Chudinova, L.P. Smolina, Zh. Neorg. Khim. 1 (1956) 1850–1856.
[11] J.C. Gallucci, R.E. Gerkin, Acta. Cryst. C 44 (1988) 1873–1876.
[12] M. Rachwalska, J.M. Janik, J.A. Janik, G. Pytasz, T. Waluta, Phys. Stat. Sol. (a) 30 (1975) K81–K82.
[13] A. Migdał-Mikuli, E. Mikuli, M. Rachwalska, S. Hodorowicz, Phys. Stat. Sol. (a) 47 (1978) 57–64.
[14] A. Migdał-Mikuli, Polimorfizm związków kompleksowych typu [Me(NH$_3$)$_6$]X$_2$ i [Me(H$_2$O)$_6$]X$_2$, ed. Uniwersytet Jagielloński, Kraków, 1995 (in polish).
[15] A. Migdał-Mikuli, E. Mikuli, S. Wróbel, Ł. Hetmańczyk, Z. Nat. 54 (10–11) (1999) 590–594.
[16] A. Migdał-Mikuli, J. Hetmańczyk, W. Nitek, E. Mikuli, Ł. Hetmańczyk, J. Mol. Struct. 891 (2008) 233–241.
[17] G.F. Smith, E.G. Koch, Z. Anogr. Chem. 223 (1935) 17–27.
[18] J. Fujita, K. Nakamoto, M. Kobayashi, J. Am. Chem. Soc. 78 (1956) 3295.
[19] E. Mikuli, A. Migdał-Mikuli, N. Górska, S. Wróbel, E. Ściesiński, J. Ściesińska, J. Mol. Struct. 519 (2003) 651–653.
[20] Y. Chen, D.H. Christensen, O.F. Nielsen, E. Pedersen, J. Mol. Struct. 294 (1993) 215–218.
[21] A. Kulczycki, Phys. Stat. Sol. (b) 103 (1981) 753–756.